Valorization of waste apple pomace for production of platform biochemicals: a Multi-objective optimization study

Oseweuba Valentine Okoro*[a], Lei Nie[b], Parinaz Hobbi[a] Amin Shavandi*[a]

[a] BioMatter unit - École polytechnique de Bruxelles, Université Libre de Bruxelles (ULB), Avenue F.D. Roosevelt, 50 - CP 165/61, 1050 Brussels, Belgium.

[b] College of Life Sciences, Xinyang Normal University (XYNU), Xinyang 464000, China.

Correspondence:

oseweubaokoro@gmail.com (O.V.O), Tel: +32 (0) 2650 3047

amin.shavandi@ulb.be (A.S), Tel: +32 (0) 2650 3047

Highlights

- Production of multiple biochemicals from pomace was assessed;
- Environmental and economic performances of the production process investigated;
- Multi-objective optimisation of the production process undertaken.

Abstract

In line with the prevailing global interest in value extraction from biomass waste streams, the current study explored the technical feasibility of valorizing waste apple pomace (WAP) to produce high-value biochemicals of 5-hydroxymethylfurfural (HMF), lactic acid, and xylitol. Technical feasibility was demonstrated via a process simulation study that employed experimental data and incorporated previously reported approaches in the literature. Economic and environmental performances of the WAP based biorefinery were assessed using the internal rate of return (IRR) and the mass of greenhouse gas emission per unit mass of feedstock (G_F) as sufficient performance indicators, respectively. The study was able to show that as the IRR value increased (better economic performance), the G_F increased (poorer environmental performance). This suggested that the determination of the optimal condition of the environmental and economic performances would require the imposition of trade-offs. The preferred trade-off condition for enhanced economic and

environmental performances was subsequently determined via multi-objective optimization, with a Pareto front containing non-dominated equally optimal solutions subsequently developed. The present work, therefore, provides an in-depth performance analysis of WAP based biorefinery as a waste management strategy. Notably, the proposed strategy of multiple product generation from biomass may be extended to other organic waste based biorefineries.

Keywords: platform-biochemicals; waste valorization; waste apple pomace; biorefinery

Statement of novelty

For the first time an efficient process design, modelling and simulation of a waste apple pomace based biorefinery for the multi production of 5-hydroxymethylfurfural, lactic acid, and xylitol is presented. Environmental and economic performance considerations were incorporated in the study with a converse relation between these performance concerns, demonstrated. Recognizing this converse relation, the trade-off between the environmental and economic performances was achieved via the application of the non-dominated sorting based multi-objective evolutionary algorithm. To the best of our knowledge, such a work exploring the use of the non-conventional high moisture feedstock of waste apple pomace as a sustainable feedstock in multi-purpose biorefinery for the production of bioproducts is yet to be explored in the literature. We therefore consider this manuscript exceptional for its

novelty and engineering creativity and anticipate that it will significantly contribute to the state of the art of biomass valorization.

1 Introduction

Throughout human history, there has never been a period characterized by a greater sustained drive toward a circular economy via the exploration of value extraction opportunities from organic waste, than the present time. Finite fossil resources are currently satisfying most of the world's chemical (~ 80%) and energy (~ 90%) demands, leading to undesirable environmental effects such as the pollution of the lands and surrounding water bodies and the emission of greenhouse gases that are responsible for the prevailing global warming challenge. There is now a consensus in the scientific community that there is a need to explore alternative and renewable carbon sources to produce carbon-neutral bioproducts and bioenergy [1]. Biomass such as agro-industrial waste, including lime and orange peel, apple pomace, wheat bran, coconut husk, can provide renewable carbon that can be converted to high-value products, via the exploration of the biorefinery concept [2]. The biorefinery concept describes the integration of biomass conversion technologies to enable biomass fractionation to their composing intermediates or macromolecules and the subsequent transformation of these macromolecules to bio-based products. Transformations in such biorefineries are typically achieved via biochemical and/or thermochemical (catalytically supported) pathways that enable the synergy of sustainable and efficient production outcomes [3, 4].

Waste apple pomace has been identified as one potential feedstock for value extraction. This pomace is generated as a consequence of the processing of fruits via milling and pressing operations for juice extraction [5, 6] and can be quite substantial more so as it constitutes about 25-30 wt.% [7] of the total mass of the apple fruit. As an illustration, consider that in Belgium alone, waste apple pomace generation from domestic apple production only (i.e., excluding waste from imported apples) can reach up to 108 ktons (i.e., ~30 wt.% of apple is the waste pomace) annually [6, 8, 9]. Additionally, in India, the waste apple pomace can reach ~1 million tons per year [10]. Recognizing the value of waste apple pomace as a possible resource, several studies have previously explored its use as a source of pectin [11] and dietary fiber [12]. Notably, its high concentration of useful polysaccharides [11, 13, 14] suggests its sufficiency as a source of sugars that may serve as renewable carbon sources for biochemical production.

The present study, therefore, seeks to explore the viability of valorizing the waste apple pomace for the production of high-value platform biochemicals of lactic acid, xylitol, and 5-(hydroxymethyl)furfural (HMF) via a multi-product waste apple pomace (WAP)-based biorefinery. These biochemicals are now discussed briefly below;

- Lactic acid ($CH_3CHCOOH$) is a chiral molecule characterized by two optical enantiomers, *l*(+) and *d*(–), and can be employed in the production of degradable polyesters such as polylactic acid (PLA), which can serve as an alternative to polyethylene terephthalate (PET) [15, 16]. Lactic acid is widely

employed in the pharmaceutical, food, and cosmetic industries [17]. Indeed, growing environmental concerns arising from the use of fossil-sourced PET suggest that it is now crucial to facilitate transitions to renewable polyesters (i.e. PLA) for enhanced sustainability [18]. This increasing interest in lactic acid has translated to a projected global lactic acid demand of 1.8 megatons by 2022 and 1.960 megatons by the year 2025 [19, 20].

- 5-Hydroxymethylfurfural (HMF) ($C_6H_6O_3$) is another leading versatile platform biochemical in the biorefinery context since its derivatives can be employed in the production of a broad range of useful products such as drugs, and polymeric materials [21, 22]. HMF, for instance, can be employed in the production of 2,5-furan dicarboxylic acid (FDCA) which is an alternative to terephthalic acid in the production of polyethylene terephthalate (PET) [23].

- Xylitol ($HO(CHOH)_3OH$) is another top value-added platform biochemical that is used in food, cosmetic, and pharmaceutical industries for the production of various products such as polyethylene glycol and ethylene glycol and is considered as one of the largest commercially produced polyols [24]. Xylitol can also be employed in the prevention of dental cavities, osteoporosis, acute otitis media, ear and upper respiratory infections. Xylitol's large application in the chewing gum industry has made it an important product, thus promoting enhanced global demand [25], as illustrated by the current estimated market

size of over 190.6 ktons/y, which is projected to attain a value of 266.5 ktons/y by the 2022 [26].

The selected biochemicals (lactic acid, HMF, and xylitol) in this study are not only platform chemicals capable of serving as building blocks for a range of products but have also been identified as among the top 30 biochemicals that can be obtained from biomass [27]. Notably, despite the considerable economic importance of the HMF, lactic acid, and xylitol and the undisputed waste management challenge of the biologically unstable WAP, there is no techno-economic analysis (TEA) for the valorization of waste apple pomace while imposing the proposed multi-product generation strategy. For the first time therefore, the current study sought to bridge the knowledge gap by investigating the TEA of a multi-product WAP-based biorefinery system optimized for enhanced environmental and economic performance outcomes. It is therefore anticipated that the proposed study will provide support for future research and biorefinery development efforts. Additionally, concerns regarding the preferred allocations of the WAP feedstock for the generation of the specified products for enhanced economic and environmental outcomes are also assessed in the present study.

2 Materials and methods

2.1 Materials

The waste apple pomace employed in the present study was modelled in accordance with the composition reported in [7] and is presented in Table 1.

Table 1: Composition of waste apple pomace [7]

Fractions	Component	Proportion (fraction)[a,b]
Water-soluble fraction		
	Glucose	0.11
	Fructose	0.27
	Sucrose	0.18
	Extracts[c]	0.05
Water-insoluble fraction		
	Pectin	0.03
	Starch	0.01
	Cellulose	0.15
	Hemicellulose	0.11
	Lignin	0.09

[a]dry weight basis, [b]normalised for the total mass fraction of 1, [c]Non-determined water-soluble fraction

The production of high-value chemicals of lactic acid, HMF and xylitol from waste apple pomace (WAP) was designed, modelled, and simulated using ASPEN plus v11. ASPEN plus is a simulation software that requires considerable knowledge of thermodynamics, chemical equipment design, and process integration to undertake successful simulations, and was selected as the preferred process simulation tool in the present study [28]. This is because, ASPEN plus possesses a robust thermodynamic foundation for accurate determination of physical properties, transport properties, and the phase behavior of reacting species [29, 30]. Furthermore, ASPEN plus can model and simulate different and complex

configurations of units such as reactors, distillation towers, heat exchangers, and compressors [28]. The properties of all chemical input have been provided via the inbuilt data library of ASPEN Plus. A review of existing literature shows that for complex solvent systems, the non-random two-liquid (NRTL) thermodynamic property method is sufficient to undertake thermodynamic property studies [31]. Indeed, the NRTL method has previously presented satisfactory results for binary and multi-component systems containing multiple polar and nonpolar components [32-34]. The NRTL thermodynamic property method was therefore selected as the preferred property method to facilitate the calculation of state parameters for chemical species.

To calculate the mass of the target products of LA, xylitol and HMF, reactors were modelled based on experimental data, reaction conversions of reacting species and reaction equations that were sourced from literature and are discussed further in section 2.2 below. The reactors were modelled using the stoichiometric reactor models (RSTOIC) in APSEN plus. Additionally pumps, turbines and compressors were modelled as isentropic units [35], with distillation processes modelled using the RADFRAC model for distillation columns in Aspen plus. The RADFRAC model facilitates the separation of highly non-ideal liquid mixtures, composed of constituents with varying boiling temperatures [36]. The design parameters for each distillation column (i.e condenser duty, number of stages, boil up rate etc.), were initially estimated using the Fenske–Underwood–Gilliland (FUG) method in Aspen plus for a more efficient simulation process [35].

2.2 Process description

A simplified process flow diagram of the proposed large-scale process is presented in Figure 1. Figure 1 shows that a fraction of the WAP (assumed feed rate 4.95 tons/h, dry basis) is used to generate hexose and pentose sugars employed for lactic acid (LA in Figure 1) production. The hexose and pentose sugars generated from the remaining fraction of the WAP are employed in HMF and xylitol production, respectively. The approach employed in determining the optimal mass allocation, x (Figure 1), of WAP will be discussed in section 2.3 of this study. For lactic acid production, Figure 1 shows that WAP is initially dewatered from 67 wt.% (typical moisture content based on Materne company data, Brussels Belgium) to 50 wt. % and then crushed and homogenized at 1 atm and a temperature of 25 ^{o}C to enhance mass transfer interactions. The electrical duties for the dewatering and homogenization of the WAP are assumed to be 2 kW per 1 m^3 of feed and 1.5 kW per ton of feed, respectively [37, 38]. All electricity duty demands are incorporated in the ASPEN plus model using Fortran commands in calculator blocks. The homogenized WAP is then subjected to hot water treatment in a pretreatment reactor to facilitate the 'de-lignination' and solubilization of the polysaccharides. The lignin fraction is transferred to the combined heat and power (CHP) plant for combustion to facilitate electricity and stream generation. This CHP system is based on a Rankine cycle, and is characterized by steam superheating as described in [39]. Briefly, in the Rankine cycle used, water is pressurized using a pump (0.9 efficiency). It is then heated using

waste heat generated from a combustion process for the generation of superheated steam. The superheated steam is then transferred to an isentropic turbine, for the generation of useful electrical work via the expansion of the pressurized superheated steam to 1 atm. The resulting hot water is then made available for reuse within the system.

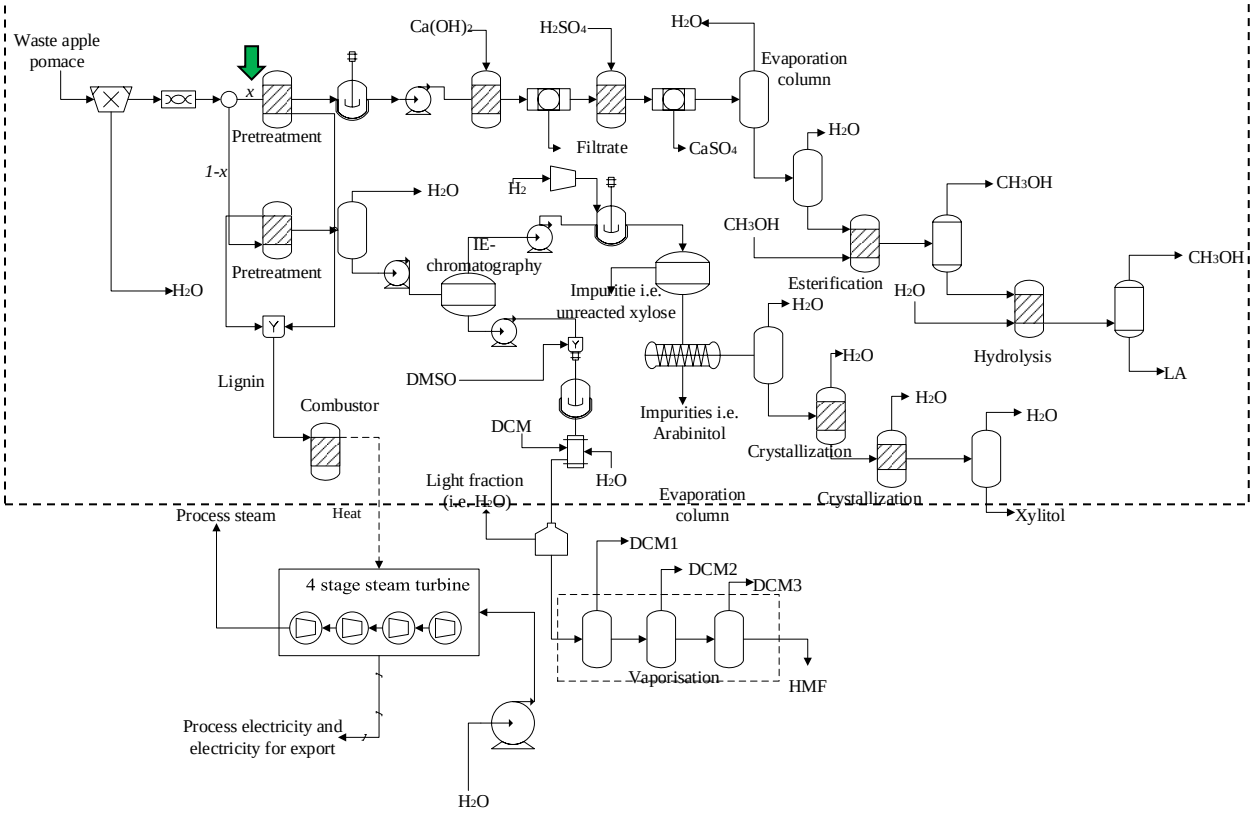

Figure 1: Simplified process flow diagram for multiproduct generation of lactic acid (LA), xylitol, and HMF from waste apple pomace (WAP). The dashed line indicates the control volume of interest and the arrow shows the allocation fraction, *x*, of the WAP.

As discussed in the literature, the hot water pretreatment approach is considered as ideal for the pretreatment of WAP feedstock since it ensures minimal losses of polysaccharides and minimizes the formation of possible inhibitory compounds such as furfural [39][40, 41]. According to previously reported experimental work, hot water pretreatment of WAP occurs at the temperature of 142.4 ^{o}C and pressure 1 atm, [42] to achieve ~65 % sugar (hexose and pentoses) recovery from the polysaccharide macromolecules present. All relevant reaction equations are presented in the supplementary document (Table S1). The resulting sugar mixture is then transferred to the fermenter, where the fermentation of both hexoses and pentoses to lactic acid is achieved using *Lactobacillus casei sub sp. rhamnous* (ATCC 10863). Iyer et al., were able to demonstrate that the microbe can completely convert hexose sugars to lactic acid [43].

On the other hand, xylose can be converted to generate a lactic acid yield of ~ 80 wt.%, at the temperature of 45 ^{o}C and pressure of 1 atm. The resulting fermentation broth is then subjected to a step-wise initial lactate precipitation treatment followed by acid treatment using $Ca(OH)_2$ and H_2SO_4 respectively. The precipitation treatment, which occurs at the temperature of 95 ^{o}C and pressure of 1 atm, facilitates the production of $C_6H_{10}CaO_6$ (calcium lactate) which is then recovered after its filtration. The $C_6H_{10}CaO_6$ is then subjected to H_2SO_4 treatment to facilitate the recovery of lactic acid and the associated generation of $CaSO_4$ (gypsum). The gypsum is then removed via filtration. The resulting lactic acid solution is then vaporized at the temperature of 100 ^{o}C to increase lactic acid concentration. Further purification of the lactic acid

is achieved via stage-wise processes of esterification, distillation, and hydrolysis [44-46]. The process of esterification is achieved using methanol to produce methyl lactate at the temperature of 100 ^{o}C and at the pressure of 1 atm followed by the distillation process to remove unreacted methanol [47]. Finally, the methyl lactate is converted to lactic acid and methanol in the hydrolysis reactor, with the resulting stream distilled to recover the methanol product, for re-use. This lactic acid purification approach facilitates the production of lactic acid with high purity levels ($\geq$ 99 wt.%) [47].

To facilitate xylitol production, the remaining mass fraction of the WAP is initially pretreated using hot water as described above. Briefly, the hydroxylate containing both hexose and pentose sugars is transferred to a column to undertake ion-exchange chromatography to separate xylose from other hexose sugars and to achieve a xylose concentration of 78 wt.% [48] [49]. The residual hexose-rich stream is employed in HMF production using methods to be discussed later below. The recovered xylose stream is converted to xylitol via catalytic hydrogenation process rather than a fermentation conversion process using methods described in [50]. This is because the catalytic hydrogenation process constitutes a more technically feasible and profitable process compared to the alternative fermentation strategy [50]. Therefore in Figure 1, the recovered xylitol is transferred to a catalytic reactor where the hydrogenation of xylose to produce xylitol is achieved using hydrogen gas at a pressure of 40 atm for 2.5 h at a temperature of 135 °C. The hydrogenation reaction is achieved under solid Raney-Ni catalyst, which is fed at a mass equivalent of 5 wt.% of the xylose [50, 51].

The product stream is then cooled to 80 °C and purified via a step-wise purification approach employing ion-exchange membranes and activated carbon columns, respectively [50]. The recovered product stream is then evaporated to increase the xylitol concentration. The xylitol solution is subjected to a two-step crystallization operation in accordance with the literature's experimental method [52]. The yield of xylitol crystal is specified as 0.81 kg xylitol / kg xylose [50, 52, 53]. Finally, the mother liquor is dried to obtain a product with a crystal purity of ≥ 98 wt. % [48]. The hexose-rich stream generated after ion-exchange chromatography highlighted above is initially vaporized to increase hexose concentration via the removal of water and low molecular weight impurities (i.e., acetic acid). The hexose-rich stream is then mixed with dimethyl sulfoxide (DMSO) solvent (H_2O/DMSO mass ratio of 1: 4 maintained) to enable the selective synthesis of HMF, then the mixture is transferred to the HMF reactor [54, 55]. In the HMF reactor, the hexose sugar (glucose) is dehydrated in acidic conditions under the action of Sn_2O/γ-Al_2O_3, with catalyst mass load of 1/1 w/w, with respect to the glucose mass, maintained, to produce HMF [54, 55]. HMF recovery from the product mixture is achieved using liquid-liquid extraction using dichloromethane (DCM) solvent. The HMF is then recovered in the organic phase (i.e. heavy fraction in Figure 1) via a three-step vapourisation process under vacuum conditions with the raffinate, recovered as the wastewater and the solvent (DCM), also recovered for re-use [54, 55]. HMF product with a purity of ≥ 96 wt.% is finally achieved.

2.3 Analysis approaches of data generated from the simulation study

In the present study, the economic performance and environmental performance of the WAP biorefinery were calculated after 'mining' mass and energy balance data obtained after the simulation process, as shown in Figure 2. Figure 2 shows that mass and energy balance results are employed as input for heat integration and equipment sizing after which relevant economic performance (IRR calculations) and environmental performance (GHG calculations) calculations are undertaken. Objective functions, based on the performance measures were subsequently optimized via multi-objective optimization methods, as shown in Figure 2.

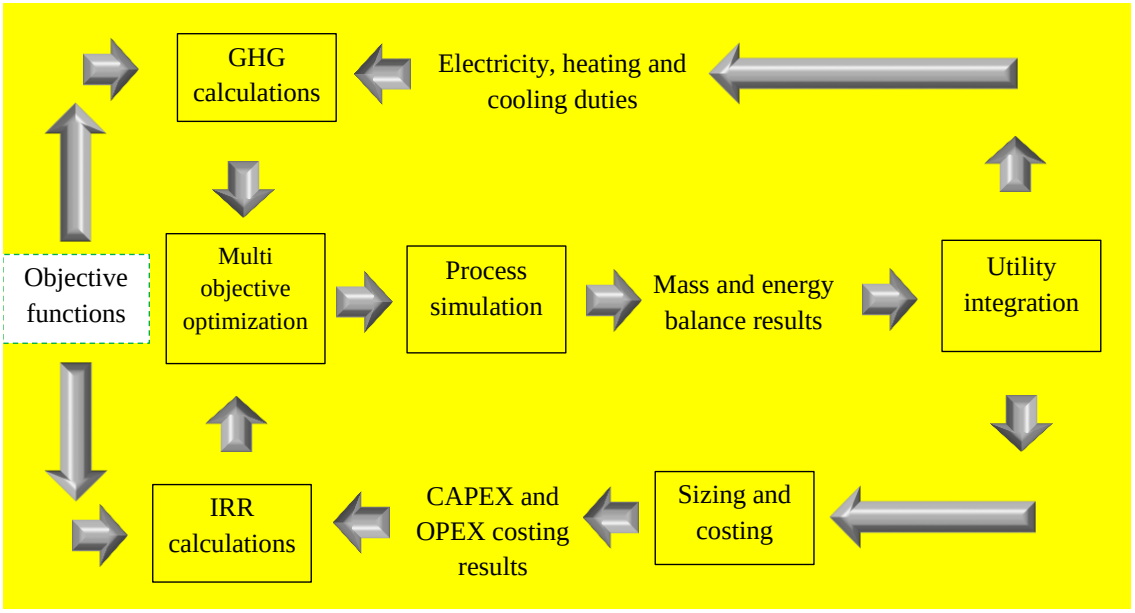

Figure 2: Simplified framework employed in the present study. CAPEX and OPEX denote the total capital investment and operating cost components, respectively.

In the present study, heat integration for energetic demand calculations in the biorefinery was calculated using the ASPEN energy analyzer v11. The ASPEN energy analyzer v11 (AEA) employs the well-known pinch point analysis to integrate heating and cooling energy requirements for all process streams. The integration of the overlap of heat flows between the "hot" and "cold" streams is highly beneficial for the sustainability of processes [35, 56, 57]. Pinch point analysis facilitates the determination of what portion of the biorefinery energetic needs, can be satisfied 'internally'. Discussions regarding the methodology and applications of pinch point analysis are outside the scope of the current study and may be found in most Engineering textbooks. In the present study, the minimum energetic duties required for the biorefinery were calculated using AEA. Having determined the minimum duties, the heating duties were assumed to be satisfied via the combustion of (externally sourced) wood pellets as a solid fuel. The cooling duties were assumed to be satisfied using a cooling tower.

The internal rate of return (IRR) was employed as the preferred economic performance metric. The IRR value refers to the discount rate, *i*, of the project when the net present value of the project equates to zero and requires the development of a discounted cash flow table [58]. The IRR was calculated as follows [59];

$$0 = \mathrm{NPV} = \sum_{n=1}^{t} \frac{R_N}{(1+i)^n} + \frac{S_n}{(1+i)^n} - \mathrm{TCI} \qquad (1)$$

where,

$$R_N = (r_t - c_t - d_t)(1 - j) + d_t \quad (2)$$

where NPV denotes the net present value in US$, R_N denotes the annual cash flow from assets in US$, TCI denotes total capital investment cost in US$, n denotes the lifetime of the project specified as 30 y; S_n denotes the salvage value, which is assumed to be zero. Additionally, r_t and c_t denote the total revenue before tax in US$ and total operating cost in US$ in year t, respectively; j and d_t denote the corporate marginal tax rate and the depreciation over the lifetime of the plant. In the present study, the minimum acceptable i value for the economic viability of WAP biorefinery plant is specified to be 10 % [60, 61].

Well-known costing correlations were employed in calculating the TCI based on the purchase costs of the equipment employed in each unit operations. The costing correlations and assumptions have been summarised in the supplementary file (Tables S2-S4). The operating cost correlations and assumptions have also been summarised in the supplementary file (Tables S5-S6). The operating cost includes fixed production cost which is maintained irrespective of the plant production capacity, and variable production cost which varies proportionately to the plant output [58, 62]. The purchase costs of most equipment such as heaters, coolers, distillation columns, pumps, and compressors employed in the biorefinery were

calculated using mapping, sizing, and costing algorithm modules of ASPEN process economic analyser v11 (APEA). The purchase costs of specialized equipment such as ion exchange columns, membrane separators, and reactors were obtained from E-commerce websites, due to the confidentially of such data from industry vendors. The calculation approaches highlighted above are consistent with the class 4 cost estimate classification system employed in engineering plant design [63, 64]. The sources (references) of prices of all chemicals in the study are also summarized in the supplementary document (Table S5) for the benefit of the reader. For consistency, inflationary effects on equipment cost sourced at different 'reference years' were considered using the chemical engineering plant cost indexes (CEPCIs) for year 2021 ($CEPCI_{2021}$) and reference year ($CEPCI_{ref}$) as follows [59] [65],;

$$P_{i,2021} = P_{i,ref}\left(\frac{\text{CEPCI}_{2021}}{\text{CEPCI}_{\text{ref}}}\right) \quad (3)$$

where $P_{i,ref}$ denotes the purchase costs for the ith equipment in the reference year; and $P_{i,2021}$ denotes the purchase costs for the ith equipment in the year 2021.

To reflect capacity effects for equipment costs at different capacities, the scaling factor approach was employed [59]. The scaling factor index was specified as 0.65 in the present study [66]. To undertake the economic assessment of the WAP biorefinery, several assumptions were also employed and are summarized in Table 2.

Table 2: Economic parameters and assumptions

Parameter	Value
Base year	2021
Project lifetime (y)	30
Plant availability (h/y)	7200
Tax rate (%)	30
Salvage value (US$)	0
Depreciation	Straight line

Having completed the economic assessment of the multi-product WAP biorefinery system, the net GHG per unit mass of feed, in kg CO_2e/kg-feed (denoted as G_F henceforth) was calculated, with 1 kg of WAP defined as the functional unit in the present study. The GHG calculation approach was employed as a surrogate measure of the environmental performance of the biorefinery. This is because, the GHG metric has been used extensively as a simplified measure of environmental performance in previous studies [56, 67, 68]. Based on the approach described in [56], the GHG generated and GHG avoided were calculated. Possible GHGs associated with microbial activity was considered negligible [56]. The net GHG per unit mass of feed (WAP) was subsequently calculated. In the present study heating utility was satisfied using wood chips as solid fuels in the onsite boiler with the associated GHG from wood pellets combustion specified as 0.015 kg/kWh[69]. For simplicity, the average GHG for electricity consumption of 0.578 kg/kWh (EU value) was employed in the

calculations [70]. Crucially also, this implies that net electricity generation onsite will aid in substantially offsetting GHG generation since GHG per kWh associated with electricity is ~39 times the GHG per kWh associated with wood pellet combustion.

2.4 Optimal WAP allocation for enhanced economics and GHG reduction potential

Based on the discussions presented so far above, it is clear that we must explore the optimization problem that involves the determination of the preferred mass fraction allocation of the WAP (i.e. x in Figure 1) that optimizes the economic and environmental performance of the biorefinery system. The IRR and G_F, therefore, constitute objective functions in the present study. Although approximately linear correlations between mass allocations of WAP and the masses of the products, are expected, nonlinear relations are anticipated between the IRR and G_F and the mass fraction allocations of WAP. This is because mass allocations of WAP present associated effects on the mass of chemical inputs, energetic profile, equipment sizes, and equipment costs. An optimization challenge is therefore presented. To resolve the optimization problem, multiple calculations, to develop a so-called simplified meta-model that presents a 'condensed' relationship between IRR and the mass fraction allocation, x, of WAP, were undertaken and an objective function developed. Similarly, the 'condensed' meta-model describing the relationship between G_F and the mass fraction allocation, x, of WAP was also developed, thus constituting another objective function. Given the possibility that the G_F and IRR may exist in competition with each other, optimization will be achieved when the mass fraction allocation, x,

that facilitates the best 'trade-off' between G_F and IRR is determined. The mathematical problem described thus far defines the multi-objective optimization challenge, and is described mathematically as follows;

$$\begin{aligned} &Max.\text{IRR} \\ &Min.G_F \end{aligned} \qquad (4)$$

Subject to

$$\begin{aligned} &x^L \le x \le x^U \\ &h(x) = 0 \\ &g(x) \le 0 \end{aligned} \qquad (5)$$

where IRR and G_F define the objective functions, $x^L \le x \le x^U$ defines the bounds on the decision variables, $h(x)=0$, and $g(x) \le 0$ define the equality and the inequality constraints respectively.

To resolve the optimization challenge, several simulation runs were undertaken for different values of x and the associated mass flows, energy flows, production costs, capital costs, G_F and IRR were subsequently calculated. The resulting multi-objective optimization problem was then solved using the non-dominated sorting-based multi-objective evolutionary algorithm (NSGA-II). NSGA-II is an algorithm that employs search methods that are modeled on natural selection, for optimization and have been used extensively in chemical engineering applications [71-73]. The algorithm

facilitates the rigorous search of different regions of a solution space leading to the determination of a diverse set of non-dominated solutions for the multi-objective optimization challenge. Discussions regarding the NSGA-II method are outside the scope of the current study and may be found elsewhere [72, 74, 75].

Crucially, however, since the NSGA-II leads to the generation of several Pareto optimal solutions, a *posteriori* preference is necessary to determine the preferred solution. In the present study, the condition that facilitates the lowest possible GHG without diminishing the IRR value to less than 10 (minimum acceptable IRR value as stated above) was considered as the optimal condition. In the present study, the NSGA-II method was executed using the Solver XL version 1.0.5.2, program. The Solver XL was utilized due to its ability to handle different variable types (i.e. integers and continuous) and its application ease. The methodology regarding cross-over and mutation schemes, population generation, and mode of operations of Solver XL may be found elsewhere [76]. Finally, the mass fraction allocation, x, of WAP that presents the optimal trade-off between G_F and IRR for optimal outcomes was subsequently determined.

3 Results and discussion

Utilizing Aspen Plus, the model of the biorefinery system which is illustrated in Figure 1 was developed and assessed for various x values. The variations of the mass of products, duty demand, G_F (net GHG per unit mass of feed), electricity generated onsite, and IRR, with values of x, are shown in Figures 3-6.

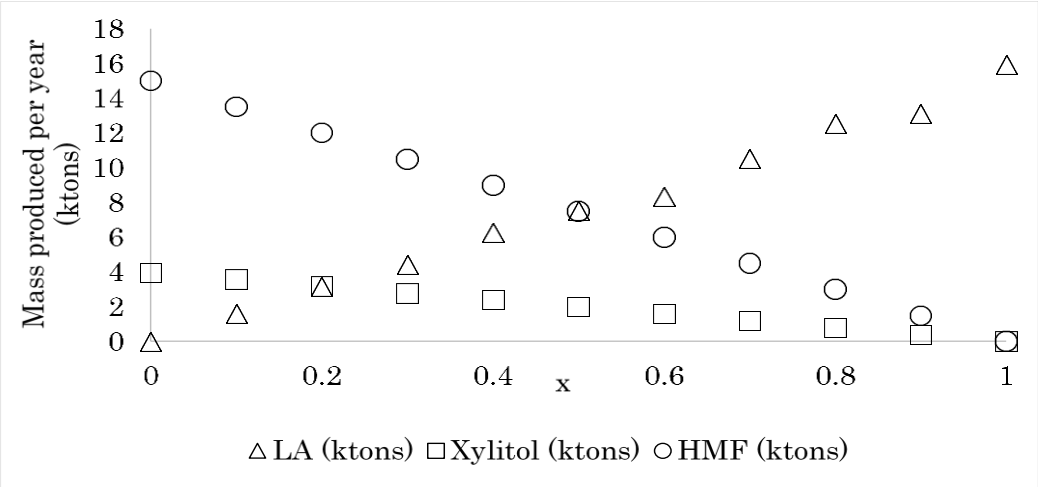

(a)

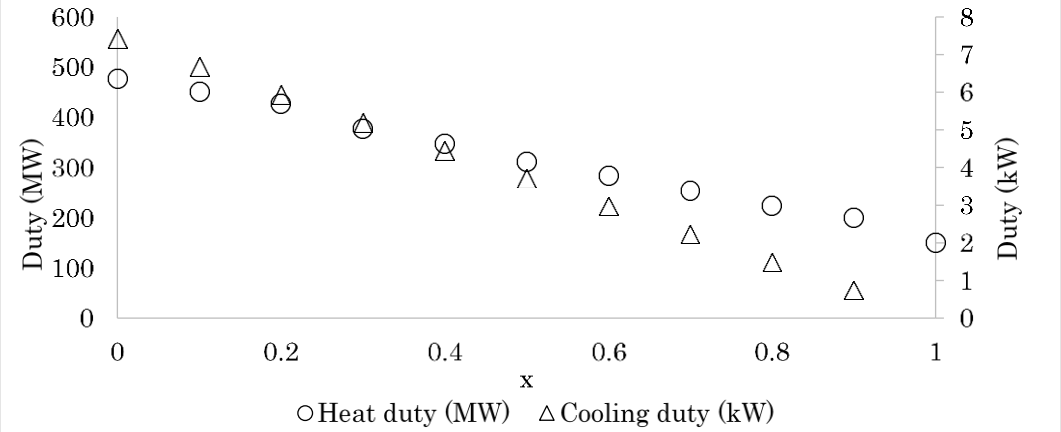

(b)

Figure 3: Variation of the mass of products generated (a) and the duty demand by the biorefinery (b) with changes in the waste apple pomace allocation fraction, *x*. LA denotes lactic acid.

Figure 3 (a) shows an inverse relationship between the masses of xylitol and HMF produced and the mass of lactic acid. This observation is expected given that higher fractions of WAP for lactic acid (i.e increasing values of *x*) diminish the mass of WAP available for conversion to xylitol and HMF. Figure 3 (a) also shows that the masses of lactic acid and HMF produced are always greater than the mass of xylitol, irrespective of the allocation fraction imposed. This is because WAP contains a lower mass fraction of hemicellulose (C5 sugar source) of 11 wt.% (dry basis) compared to the combined mass fractions of C6 sugar sources of ~ 76.7 wt.% (dry basis) of cellulose, starch, fructose and glucose present, indicating that a lower mass of C5 sugars are available for xylitol production. The energetics of the biorefinery as the allocation fraction varies were also determined as shown in Figure 3 (b). Figure 3 (b) shows that as the waste apple pomace allocation fraction, *x*, (allocation for lactic acid production) increases, the heating and cooling duties decrease. This observation indicates that the energy requirement for the lactic acid production process is less than the combined duties for the HMF and xylitol production processes.

Figure 4 also shows that net electricity generated onsite increases as the allocation fraction, *x* increases, which is reflective of the reduction in high energy demand for the compression (i.e. pressure requirement of 40 atm) of large masses of hydrogen gas during xylose hydrogenation to xylitol.

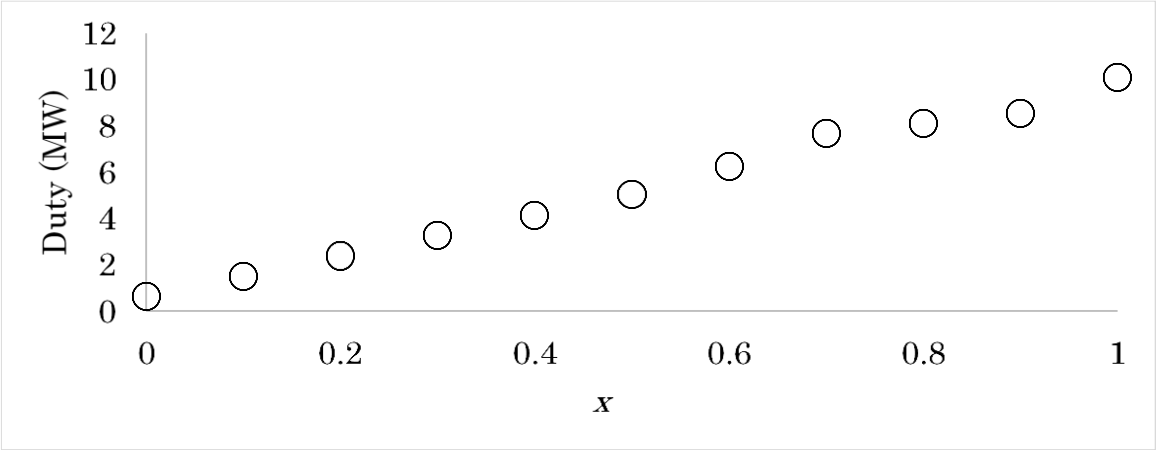

Figure 4: Variation of the net electricity generated onsite with changes in the waste apple pomace, allocation fraction, *x*.

Employing the energetic results and the GHG calculation approach discussed in section 2.3 above, the variation of the net GHG generated per unit mass of feed (G_F) with changes in the waste apple pomace allocation fraction, *x*, were calculated and are shown in Figure 5 (a). Figure 5 (a) shows that lower G_F values, indicating favorable environmental outcomes, are observed for higher values of the allocation fraction, *x*, such that for the situation of $x \geq 0.8$, negative G_F values are observed. The negative G_F value indicates that the GHG generated onsite from the combustion of externally sourced wood pellets is now less than the GHG avoided via electricity generation (from CHP) onsite. This observation is not unexpected since the net energy demand of the combined processes for HMF and xylitol production is higher than the net energy demand for the lactic acid production process, which translates to lower GHG emissions as the allocation fraction, *x*, increases.

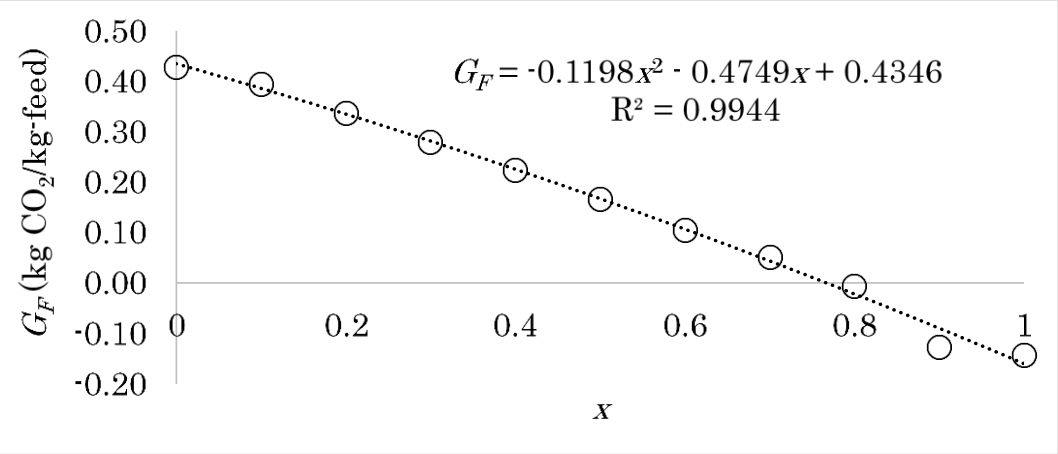

Figure 5: Variation of the net greenhouse gases generated per unit mass of feed (G_F)

Table 3: Economic outcomes for different allocation fraction of waste apple pomace

Allocation fraction x	Total capital investment (MUS$)	Operating cost (MUS$)
0	63.91	20.56
0.1	69.23	21.32
0.2	69.89	21.51
0.3	70.22	21.69
0.4	70.34	21.87
0.5	70.29	21.94
0.6	70.08	22.14
0.7	69.69	22.42

0.8	69.08	22.60
0.9	68.12	23.35
1	54.62	23.45

Assessing the total capital investment and operating costs of the biorefinery and utilizing the methods described in section 2.3 above, Table 3 summarizes the capital and the operating cost obtained for different allocation fractions *x*. Table 3 shows that the capital cost is lowest at the extremes (i.e *x*= 0 or *x*=1) which is not entirely unexpected given that only a portion of the processing capacity is employed (i.e either the lactic acid or the HMF+xylitol production process is 'cut-off'). Furthermore, the capital cost was observed to peak when the *x*=0.4. Table 3 also shows that the operating cost increases as the *x* increases, indicating that the operating cost for the combined HMF and xylitol production process is higher than the operating cost of the lactic acid production process. Next, the resulting IRR values are presented in Figure 6.

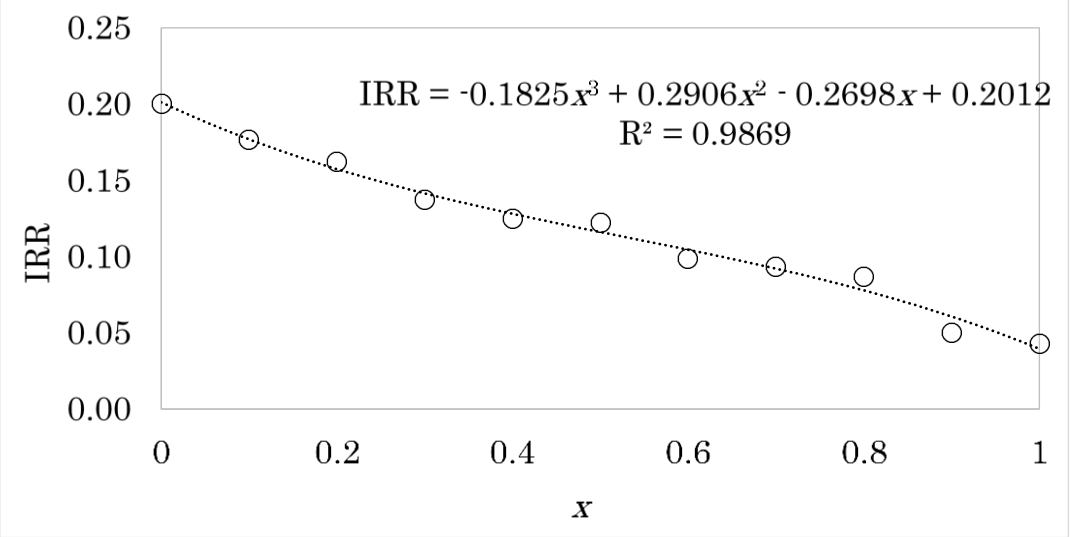

Figure 6: Variation of internal rate of return (IRR) with changes in the waste apple pomace allocation fraction, *x*.

Figure 6 shows that an opposite trend to Figure 5 is observed when the calculated IRR values are considered. This is because Figure 6 and Figure 5 show that higher values of the allocation fraction, *x* results in reduced IRR values and thus poorer economic performance, while simultaneously facilitating favorable environmental performance (i.e. lower G_F) in Figure 5. In other words, while higher values of the allocation fraction enhance environmental outcomes as illustrated by lower G_F values, higher allocation fractions lead to lower economic performances, thus presenting a conundrum regarding the apple pomace allocation fraction that leads to a suitable compromise between the competing objective functions. This problem was solved using a non-dominated Pareto plot generated using the NSGA-II as shown in Figure 7.

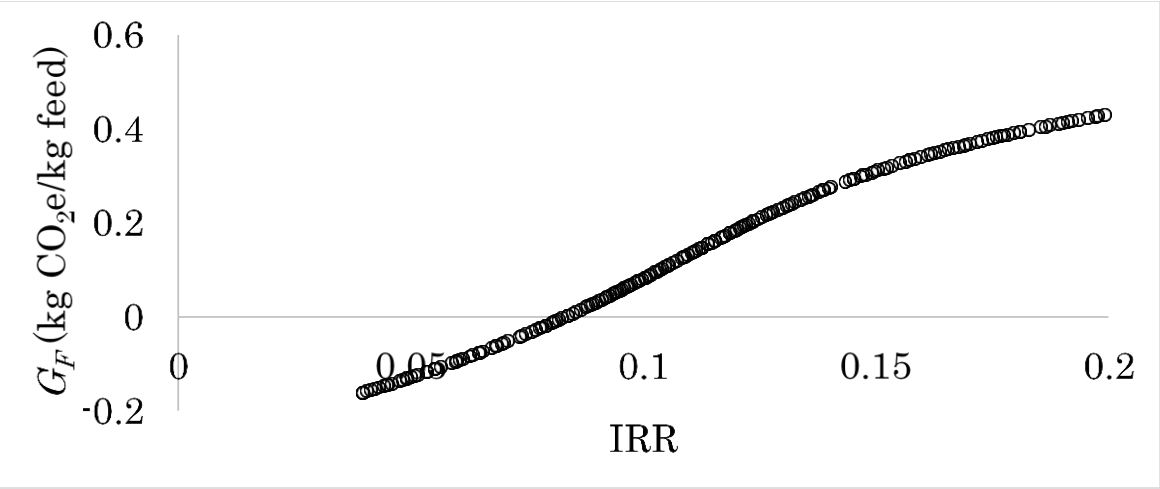

Figure 7: Pareto plot highlighting non-dominated optimal solutions (net greenhouse gases generated per unit mass of feed (G_F) vs internal rate of return (IRR))

Figure 7 shows the Pareto-optimal front that was obtained for maximizing IRR and minimizing G_F using the Solver XL program. Notably, all points on the Pareto-front are recognized as equally optimal solutions (section 2.3). Figure 6 shows that higher IRR values (i.e. favorable economics) lead to higher G_F (poor environmental performance), thus revealing the need for a trade-off. This is because optimizing the IRR will lead to the inevitable maximization of unwanted GHG emissions. Conversely, reducing GHG emissions results in negative effects on the economics of the WAP biorefinery.

Given the study specific objective to minimize the GHG without diminishing the IRR to levels lower than the minimum acceptable IRR value of 10 % (0.1), the preferred allocation fraction, x, was determined to be 0.64 (from Figure 7). This implies that to

avoid unfavorable environmental outcomes while maintaining a minimum acceptable IRR value of 10 %, 0.64 mass fraction of the WAP must be processed to lactic acid while 0.36 mass fraction of the WAP must be processed to HMF (from C6 sugars) and xylitol (from C5 sugars). Under this optimal condition the yield of the products, the capital and operating costs components of the biorefinery are summarized in Table 4.

Table 4: Outcome of the economic assessment for biorefinery at optimum condition

Parameters	Values
Fixed capital investment (MUS$)	66.65
Working capital investment (MUS$)	3.33
Total capital investment (MUS$)	69.98
Fixed operating cost (MUS$)	3.77
Variable operating cost (MUS$)	18.52
Total operating cost (MUS$)	22.29
Yield of lactic acid (wt. %, dry basis)	26.6
Yield of xylitol produced (wt. %, dry basis)	4.1
Yield of HMF produced (wt. %, dry basis)	15.4

MUS$ denotes million US$

As expected the total capital investment (total operating cost) of MUS$ 69.98 (MSU$ 22.29) for the biorefinery when x=0.64 is between the total capital investment (total operating cost) of MUS$70.1 (MUS$ 22.14) when x=0.6 and MUS$69.7 (MUS$ 22.4)

when x=0.7. The IRR and G_F values determined from Pareto-optimal front were subsequently compared to the ASPEN simulated IRR and G_F values for x =0.64 and the results shown in Table 5.

Table 5: Optimal solution based on the optimal condition of x=0.64

Objectives	Pareto optimal solution	ASPEN simulation result	Relative error
IRR	10.01	10.3	0.030
G_F (CO_2e/kg-Feed)	0.08	0.082	0.025

Table 5 shows that the results from the Pareto front and the ASPEN simulation agree, thus further reinforcing the accuracy of the simplified meta-models developed and employed as objective functions in the optimization study. Table 5 also shows that if the minimum acceptable IRR value of 10% is to be maintained, then the G_F cannot be lower than ~0.08 CO_2e/kg-feed.

4 Real-life implications of this study

Having determined that the preferred economic performance and environmental performance values were when the IRR was 10 % and G_F value was ~0.08 CO_2e/kg-feed, the associated benefits of undertaking the WAP valorization to produce HMF, lactic acid and xylitol are highlighted using Figure 8.

Figure 8 shows that apart from the opportunity to produce high value biochemicals of lactic acid, HMF and xylitol from WAP, the proposed biorefinery presents an

opportunity for an improved environmental outcome relative to the conventional WAP management approach. This is because the GHG emission per kg of WAP can be reduced by ~28% relative to the GHG emission per kg of WAP disposal to landfills of 0.112 kg CO_2e [77].

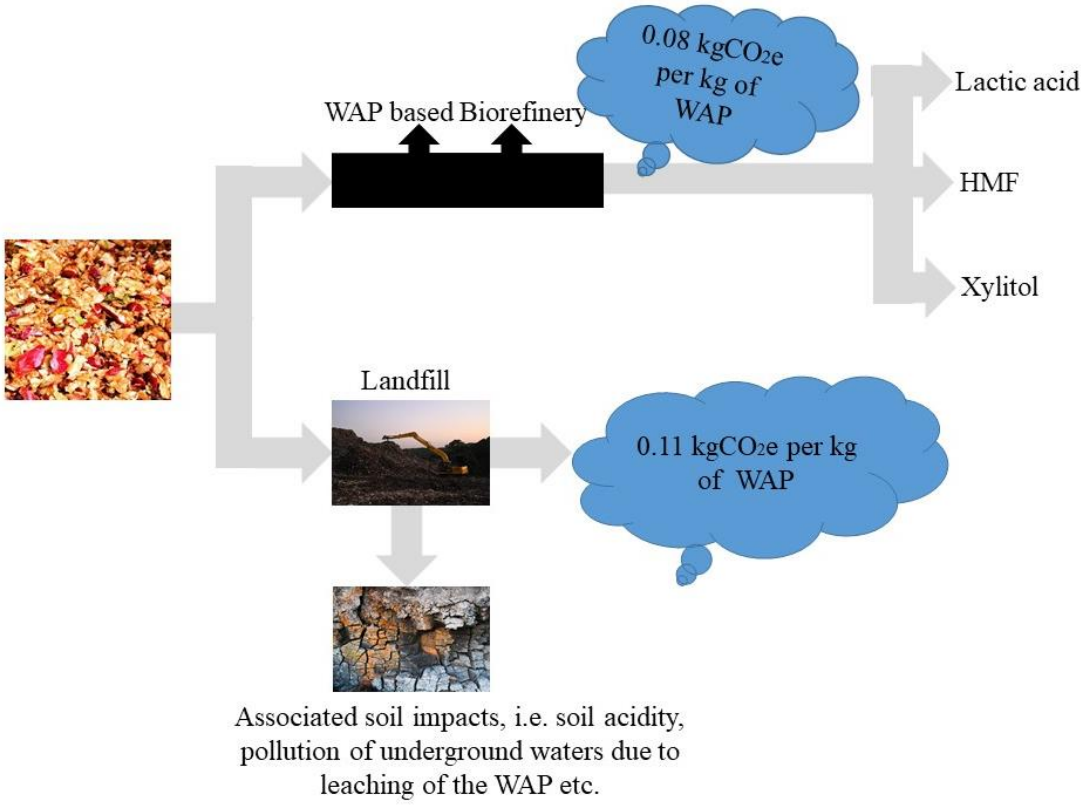

Figure 8: Biorefinery pathway for waste apple pomace (WAP) management via the biorefinery approach compared to the conventional landfill approach

Notably apart from the GHG emission (i.e., air pollution effects), Figure 8 also shows that the disposal of the WAP in landfills can increase soil acidity and increase the risk of polluting underground water bodies. It should also be noted that in both cases (i.e. biorefinery and landfill), the emissions reported did not include emissions

accrued from the transportation of the waste apple pomace stream. It must therefore be emphasized that the results presented herein may only serve as the basis for preliminary decisions regarding the environmental and economic impacts of the exploration of the WAP based biorefinery system. This is because, the GHG metric used in the present study does not provide a basis for making widespread systematic generalizations, more so as emissions due to other activities such as the transportation of the WAP and wood chips to the biorefinery site, have not been considered. The sequel of this study will explore a comprehensive 'cradle to grave' life cycle assessment study, as a basis of providing improved and universal environmental performance results.

5 Conclusion.

This study has presented an assessment of the net greenhouse gas (GHG) emission (kg) per unit mass (kg) of feedstock, denoted as G_F, and the internal rate of return, denoted as IRR, as surrogate measures of environmental performance and economic performance of a waste apple pomace (WAP) based biorefinery system. The WAP biorefinery was assessed for the scaled-up recovery of valuable platform biochemicals of lactic acid, xylitol and 5-(hydroxymethyl)furfural from WAP. Given the multi-product status of the biorefinery, it was crucial to determine the appropriate allocation fraction, x, of the WAP to provide, C5 and C6 sugars for lactic acid production, with the residual fraction $(1-x)$ of the WAP, providing C5 sugars for xylitol production and C6 sugars for HMF production. Several allocation fractions were therefore assessed in the present study, with the associated economic and

environmental performances for each allocation fraction calculated. The study was able to demonstrate that a converse relationship exists between environmental performance and economic performance of the WAP based biorefinery. Recognizing this converse relationship, it was necessary to determine the optimal trade-off of the objectives via the imposition of a multi-objective optimization strategy. In the present study, therefore, a non-dominated sorting-based multi-objective evolutionary algorithm (NSGA-II) was employed in undertaking a rigorous search of solution space to determine a diverse set of optimal solutions on a Pareto-optimal plot. The optimal trade-off of the objectives was subsequently specified as the condition that facilitated the lowest environmental cost (i.e lowest G_F) without compromising the minimum acceptable condition for economic acceptability, specified as the IRR of 10 %, in the present study. Notably, at the specified compromise solution, the environmental performance of the biorefinery was shown to compete favorably with the environmental performance of the conventional landfill waste apple pomace management approach, since the utilization of the biorefinery led to reduced specific GHG emissions overall.

6 Acknowledgments

The first author gratefully acknowledges the financial support of Wallonia-Brussels International via the Wallonie-Bruxelles International (WBI) excellence Postdoctoral fellowship. Materne company is also acknowledged for their expert information input.

7 Declarations

Funding: This research received no external funding.

Conflicts of Interest: The authors declare no conflict of interest in this study.

References

1. Fernando, S., et al., *Biorefineries: current status, challenges, and future direction.* 2006. **20**(4): p. 1727-1737.
2. Okoro, O.V., Z. Sun, and J. Birch, *Meat processing waste as a potential feedstock for biochemicals and biofuels – A review of possible conversion technologies.* Journal of Cleaner Production, 2017. **142**: p. 1583-1608.
3. Hingsamer, M. and G. Jungmeier, *Chapter Five - Biorefineries*, in *The Role of Bioenergy in the Bioeconomy*, C. Lago, N. Caldés, and Y. Lechón, Editors. 2019, Academic Press. p. 179-222.
4. Okoro, O.V. and Z. Sun, *The characterisation of biochar and biocrude products of the hydrothermal liquefaction of raw digestate biomass.* Biomass Conversion and Biorefinery, 2020.
5. Kosseva, M.R., *Chapter 3 - Sources, Characterization, and Composition of Food Industry Wastes*, in *Food Industry Wastes*, M.R. Kosseva and C. Webb, Editors. 2013, Academic Press: San Diego. p. 37-60.
6. Kruczek, M., B. Drygaś, and C.J.W.S.N. Habryka, *Pomace in fruit industry and their contemporary potential application.* 2016. **48**: p. 259-265.
7. Gustafsson, J., et al., *Development of Bio-Based Films and 3D Objects from Apple Pomace.* Polymers, 2019. **11**(2): p. 289.
8. Carunchia, M., L. Wang, and J.H. Han, *19 - The use of antioxidants in the preservation of snack foods*, in *Handbook of Antioxidants for Food Preservation*, F. Shahidi, Editor. 2015, Woodhead Publishing. p. 447-474.
9. Koen, v.G., *Apple production in Belgium from 2005/06 to 2019/2020*. 2021, Statista.
10. Shalini, R. and D.K. Gupta, *Utilization of pomace from apple processing industries: a review.* Journal of food science and technology, 2010. **47**(4): p. 365-371.
11. Yates, M., et al., *Multivalorization of apple pomace towards materials and chemicals. Waste to wealth.* Journal of Cleaner Production, 2017. **143**: p. 847-853.
12. Bhushan, S. and M. Gupta, *Apple Pomace: Source of Dietary Fibre and Antioxidant for Food Fortification*, in *Handbook of Food Fortification and Health: From Concepts to Public Health*

Applications Volume 2, V.R. Preedy, R. Srirajaskanthan, and V.B. Patel, Editors. 2013, Springer New York: New York, NY. p. 21-27.
13. Lyu, F., et al., *Apple Pomace as a Functional and Healthy Ingredient in Food Products: A Review.* Processes, 2020. **8**(3).
14. Antonic, B., et al., *Apple pomace as food fortification ingredient: A systematic review and meta-analysis.* J Food Sci, 2020. **85**(10): p. 2977-2985.
15. Abdel-Rahman, M.A., Y. Tashiro, and K. Sonomoto, *Recent advances in lactic acid production by microbial fermentation processes.* Biotechnology Advances, 2013. **31**(6): p. 877-902.
16. Dusselier, M., et al., *Toward Functional Polyester Building Blocks from Renewable Glycolaldehyde with Sn Cascade Catalysis.* ACS Catalysis, 2013. **3**(8): p. 1786-1800.
17. Dagher, S.F., et al., *Chapter 5 - Cell Immobilization for Production of Lactic Acid: Biofilms Do It Naturally*, in *Advances in Applied Microbiology*. 2010, Academic Press. p. 113-148.
18. E4tech, *UK Top Bio-based Chemicals Opportunities*. 2017, E4tech: London.
19. BusinessWire, *Global Lactic Acid Market 2017-2025 - Growth Trends, Key Players, Competitive Strategies and Forecasts - Research and Markets*. 2017.
20. Azaizeh, H., et al., *Production of Lactic Acid from Carob, Banana and Sugarcane Lignocellulose Biomass.* Molecules, 2020. **25**(13).
21. Román-Leshkov, Y., J.N. Chheda, and J.A. Dumesic, *Phase modifiers promote efficient production of hydroxymethylfurfural from fructose.* Science, 2006. **312**(5782): p. 1933-7.
22. Zhou, C., et al., *Conversion of glucose into 5-hydroxymethylfurfural in different solvents and catalysts: Reaction kinetics and mechanism.* Egyptian Journal of Petroleum, 2017. **26**(2): p. 477-487.
23. Motagamwala, A.H., et al., *Toward biomass-derived renewable plastics: Production of 2, 5-furandicarboxylic acid from fructose.* 2018. **4**(1): p. eaap9722.
24. Delgado Arcaño, Y., et al., *Xylitol: A review on the progress and challenges of its production by chemical route.* Catalysis Today, 2020. **344**: p. 2-14.
25. Venkateswar Rao, L., et al., *Bioconversion of lignocellulosic biomass to xylitol: An overview.* Bioresour Technol, 2016. **213**: p. 299-310.
26. Industryexperts *Xylitol – A Global Market Overview*. 2017.
27. Werpy, T., et al., *Results of screening for potential candidates from sugars and synthesis gas.* 2004. **1**: p. 76.
28. Alnur, A., et al., *Simulation of xylitol production: a review.* 2013. **7**(5): p. 366-372.
29. Schefflan, R., *Teach yourself the basics of Aspen Plus*. 2011: Wiley Online Library.
30. Okoro, O.V., Z. Sun, and J. Birch, *Techno-Economic Assessment of a Scaled-Up Meat Waste Biorefinery System: A Simulation Study.* 2019. **12**(7): p. 1030.
31. Marcotullio, G., *The chemistry and technology of furfural production in modern lignocellulose-feedstock biorefineries.* 2011.
32. Peña-Tejedor, S., et al., *Vapor–liquid equilibria and excess volumes of the binary systems ethanol+ ethyl lactate, isopropanol+ isopropyl lactate and n-butanol+ n-butyl lactate at 101.325 kPa.* 2005. **230**(1-2): p. 197-203.
33. Deterre, S., et al., *Vapor–liquid equilibria measurements of bitter orange aroma compounds highly diluted in boiling hydro-alcoholic solutions at 101.3 kPa.* 2012. **57**(12): p. 3344-3356.
34. Vu, D.T., et al., *Vapor− liquid equilibria in the systems ethyl lactate+ ethanol and ethyl lactate+ water.* 2006. **51**(4): p. 1220-1225.
35. Petersen, A.M., et al., *Evaluating refinery configurations for deriving sustainable aviation fuel from ethanol or syncrude.* Fuel Processing Technology, 2021. **219**: p. 106879.
36. ASPEN-plus, *Aspen Plus User Guide*. 2000, ASPEN technology incorporated: Cambridge.

37. Alibaba. *Mechanical Dewatering device* 2021 February/18/2021 February/18/2021]; Available from: https://www.alibaba.com/product-detail/Dewatering-Dewatering-Machine-NORSEN-Vehicular-Sludge_1600051333912.html?spm=a2700.galleryofferlist.normal_offer.d_title.5c49383dKmOCni&s=p.
38. Zimmer, E., *Optimal use of resources and energy during fruit juice extraction*. 2017, Fruit Processing: Nlederwenlngen.
39. Okoro, O.V. and A. Shavandi, *An assessment of the utilization of waste apple slurry in bio-succinic acid and bioenergy production.* International Journal of Environmental Science and Technology, 2021.
40. Kim, D., *Physico-Chemical Conversion of Lignocellulose: Inhibitor Effects and Detoxification Strategies: A Mini Review.* Molecules, 2018. **23**: p. doi:10.3390/molecules23020309.
41. Pérez, J.A., et al., *Optimizing Liquid Hot Water pretreatment conditions to enhance sugar recovery from wheat straw for fuel-ethanol production.* Fuel, 2008. **87**(17): p. 3640-3647.
42. Hijosa-Valsero, M., A.I. Paniagua-García, and R. Díez-Antolínez, *Biobutanol production from apple pomace: the importance of pretreatment methods on the fermentability of lignocellulosic agro-food wastes.* Applied microbiology and biotechnology, 2017. **101**(21): p. 8041-8052.
43. Iyer, P.V., S. Thomas, and Y. Lee. *High-yield fermentation of pentoses into lactic acid*. in *Twenty-First Symposium on Biotechnology for Fuels and Chemicals*. 2000. Springer.
44. Su, C.-Y., et al., *Control of Highly Interconnected Reactive Distillation Processes: Purification of Raw Lactic Acid by Esterification and Hydrolysis.* Industrial & Engineering Chemistry Research, 2015. **54**(27): p. 6932-6940.
45. Kamble, S.P., et al., *Purification of Lactic Acid via Esterification of Lactic Acid Using a Packed Column, Followed by Hydrolysis of Methyl Lactate Using Three Continuously Stirred Tank Reactors (CSTRs) in Series: A Continuous Pilot Plant Study.* Industrial & Engineering Chemistry Research, 2012. **51**(4): p. 1506-1514.
46. Lee, H., *Development of lactic and succinic acid biorefinery configurations for integration into a thermomechanical pulp mill*. 2015, École Polytechnique de Montréal.
47. Kumar, R., et al., *A continuous process for the recovery of lactic acid by reactive distillation.* 2006. **81**(11): p. 1767-1777.
48. Melaja, A. and L. Hämäläinen, *US-patent : Process for making xylitol*. 1977. p. 285.
49. Özüdoğru, H.M.R., et al., *Techno-economic analysis of product biorefineries utilizing sugarcane lignocelluloses: Xylitol, citric acid and glutamic acid scenarios annexed to sugar mills with electricity co-production.* Industrial Crops and Products, 2019. **133**: p. 259-268.
50. Mountraki, A., et al., *Selection of biorefinery routes: the case of xylitol and its integration with an organosolv process.* 2017. **8**(7): p. 2283-2300.
51. Mikkola, J.-P., T. Salmi, and R. Sjöholm, *Modelling of kinetics and mass transfer in the hydrogenation of xylose over Raney nickel catalyst.* 1999. **74**(7): p. 655-662.
52. Martínez, E.A., et al., *Batch cooling crystallization of xylitol produced by biotechnological route.* 2009. **84**(3): p. 376-381.
53. Wang, Z., et al., *Measurement and correlation of solubility of xylitol in binary water+ethanol solvent mixtures between 278.00 K and 323.00K.* Korean Journal of Chemical Engineering, 2013. **30**(4): p. 931-936.
54. Kougioumtzis, M.A., et al., *Production of 5-HMF from cellulosic biomass: Experimental results and integrated process simulation.* 2018. **9**(12): p. 2433-2445.
55. Santiago, B.S. and R.J.C.E.T. Guirardello, *5-hydroxymethylfurfural Production in a Lignocellulosic Biorefinery: Techno-economic Analysis.* 2020. **80**: p. 139-144.

56. Petersen, A.M., et al., *Evaluation of Biorefining Scenarios for Advanced Fuels Production from Triticale Grain.* Energy & Fuels, 2020. **34**(9): p. 11003-11013.
57. Okoro, O.V., Z. Sun, and J.J.S. Birch, *Catalyst-free biodiesel production methods: A comparative technical and environmental evaluation.* 2018. **10**(1): p. 127.
58. Okoro, O.V. and F.D.J.A. Faloye, *Comparative assessment of thermo-syngas fermentative and liquefaction technologies as waste plastics repurposing strategies.* 2020. **2**(3): p. 378-392.
59. Okoro, O.V., A.N. Banson, and H.J.C. Zhang, *Circumventing Unintended Impacts of Waste N95 Facemask Generated during the COVID-19 Pandemic: A Conceptual Design Approach.* 2020. **4**(3): p. 54.
60. Kumar, D., S.P. Long, and V.J.G.B. Singh, *Biorefinery for combined production of jet fuel and ethanol from lipid-producing sugarcane: a techno-economic evaluation.* 2018. **10**(2): p. 92-107.
61. García Haro, P., *Thermochemical Biorefineries and based on DME as platform chemical: conceptual design and technoeconomic assessment. Biorrefinerías Termoquímicas basadas en DME como intermediario: Diseño conceptual y análisis tecno-económico.* 2013.
62. Towler, G. and R. Sinnott, *Chemical engineering design: Principles, Practice and Economics of Plant and Process Design*. 2008, Amsterdam: Elsevier.
63. Lange, J.-P.J.C., *Fuels and chemicals manufacturing; guidelines for understanding and minimizing the production costs.* 2001. **5**(2): p. 82-95.
64. Christensen, P., et al., *Cost Estimate Classification system-as applied in engineering, procurement, and construction for the process industries.* 2005. **2011**.
65. Chemical-Enginerring, *CEPCI*. 2021.
66. Spath, P., et al., *Biomass to hydrogen production detailed design and economics utilizing the Battelle Columbus Laboratory indirectly-heated gasifier*. 2005, National Renewable Energy Lab., Golden, CO (US).
67. Doka, G., *Final report ecoinvent: Life cycle inventories of waste treatment services*, in *ecoinvent report No. 13*. 2003: Dübendorf.
68. Hedemann, J., et al., *Technical documentation of the ecoinvent database.* 2007. **2**.
69. Forest-research, *Carbon emissions of different fuels*. 2021.
70. CES-MED, *Technical annex to the SEAP template instructions document: THE EMISSION FACTORS*. 2015, Cleaner enrgy saving mediterranean cities.
71. Rangaiah, G.P., Z. Feng, and A.F.J.P. Hoadley, *Multi-objective optimization applications in chemical process engineering: Tutorial and review.* 2020. **8**(5): p. 508.
72. Srinivas, N. and K.J.E.c. Deb, *Muiltiobjective optimization using nondominated sorting in genetic algorithms.* 1994. **2**(3): p. 221-248.
73. Chaudhari, P. and S.K. Gupta, *Multiobjective Optimization of a Fixed Bed Maleic Anhydride Reactor Using an Improved Biomimetic Adaptation of NSGA-II.* Industrial & Engineering Chemistry Research, 2012. **51**(8): p. 3279-3294.
74. Deb, K., et al. *A fast elitist non-dominated sorting genetic algorithm for multi-objective optimization: NSGA-II*. in *International conference on parallel problem solving from nature*. 2000. Springer.
75. Deb, K., *Multi-objective optimisation using evolutionary algorithms: an introduction*, in *Multi-objective evolutionary optimisation for product design and manufacturing*. 2011, Springer. p. 3-34.
76. SolverXL, *SolveXL - Genetic Algorithm Optimization add-in for Microsoft Excel*. 2013.
77. Gassara, F., et al., *Pomace waste management scenarios in Québec—Impact on greenhouse gas emissions.* Journal of Hazardous Materials, 2011. **192**(3): p. 1178-1185.